

Epistemic Horizon Minority Games: When Abundance Reduces Strategic Value

Faruk Alpay* Levent Sarioğlu

Department of Computer Engineering, Bahçeşehir University, Istanbul, Türkiye
{faruk.alpay, levent.sarioglu}@bahcesehir.edu.tr

Abstract

Strategic value can fall when an option becomes visible. A route, signal, bet, or opportunity may be attractive because few agents see it; public attention can erase the advantage it reveals. We formalize this mechanism as an epistemic-horizon minority game (EHMG), where agents have bounded observation horizons, action-specific awareness, desire-biased utilities, and payoffs that decline with crowding. The object is not a fixed congestion game with omitted actions, but an awareness-transition game on a finite lattice. We prove fixed-awareness potential-game reduction, finite monotone awareness convergence, logit mean-field uniqueness under an explicit norm condition, non-reducibility from static count-based congestion games, and sensitivity bounds for nonlinear revelation. We separate the target price of information from aggregate welfare loss, showing that they can coincide, diverge, or recommend opposite disclosure policies. Private revelation, public common revelation, and correlated group disclosure are modeled as distinct signal structures with different equilibrium effects. Experiments regenerate awareness sweeps, public visibility shocks, horizon–desire grids, information-constrained Braess examples, disclosure optimization, minimum harmful revelation, and counterfactual baselines isolating the epistemic mechanism from ordinary full-awareness congestion. Strategic trace encodings are evaluated as a controlled regime-recognition benchmark: raw trajectories, Fourier summaries, recurrence and Gramian images, image bundles, local-filter features, leakage probes, phase-scrambled controls, resolution and recurrence-threshold sweeps, spectral carriers, and IAAFT matched-null parameter-shift controls test whether trace encodings recover strategic structure under robust nulls.

1 Introduction

In ordinary language, abundance suggests value. In strategic systems this intuition often fails. If a bar is enjoyable only when few people attend, a forecast that the bar will be empty can make it crowded. If a route is faster only when few drivers take it, public route guidance can erase its advantage. If a bet is attractive because a player wants a particular hand to win, the player’s own desire can leak into the perceived probability of success. In each case, value is not attached to the object alone. It is attached to how many agents see the object, how many desire it, and what each agent believes others will do.

The El Farol bar problem was introduced by Arthur as a compact model of inductive reasoning under bounded rationality [2, 3]. Challet and Zhang’s minority game placed the same intuition into a game form in which agents benefit from being on the less crowded side [7, 24]. Congestion games formalize the general case in which an action’s payoff is a decreasing function of the number of users

*Corresponding author: alpay@lightcap.ai

[19]. Braess’ paradox shows that adding an option to a decentralized network can make everyone worse off [5, 16]; informational Braess shows that additional information about options can also be harmful [1]. These literatures capture one part of the intuition: more access can reduce value.

The missing part is epistemic. Agents do not choose in the world as a whole; they choose inside an observation horizon. A person walking through a forest can be locally coherent while omitting most simultaneous events from the decision model. A gambler can know that an event is random while still shifting a borderline prediction toward the wanted outcome. A community can disagree about an unobservable domain not merely because agents assign different probabilities, but because their state spaces do not contain the same objects. Epistemic game theory makes beliefs, higher-order beliefs, common knowledge, and unawareness formal objects [4, 12, 18, 21]. Behavioral decision theory adds the empirical fact that desire and risk framing can distort judgment [8, 13, 20, 23].

This paper combines these two sides. We introduce an *epistemic horizon minority game* (EHMG), a repeated negative-frequency game in which each agent has a bounded memory horizon and a possibly incomplete action set. An action can be physically available but absent from an agent’s awareness. When the action is revealed, it may gain demand because it is newly visible, but lose payoff because its prior advantage was epistemic scarcity.

Contributions.

- We define EHMGs with awareness sets, observation horizons, desirability-biased perceived utilities, and realized payoffs that decline with action crowding.
- We introduce an awareness lattice and transition operators for private, public, and correlated revelation; this yields a mean-field awareness equilibrium object and finite convergence result for monotone awareness expansion.
- We prove a theorem family for visibility: fixed-awareness EHMGs reduce to potential games, but awareness transitions create non-reducible comparative statics; under logit contraction the mean-field equilibrium is unique and its price of information is bounded for nonlinear congestion.
- We embed the Braess comparison inside EHMG as an information-constrained Wardrop instance rather than using it only as an analogy.
- We define algorithmic disclosure tasks, including budgeted welfare-safe disclosure and minimum harmful revelation, and give exact, greedy, oracle, and treewidth-oriented computational baselines.
- We materialize counterfactual experiments against ordinary congestion, full-awareness minority dynamics, partial revelation, and no-scarcity-bonus controls.
- We adapt a reusable algorithmic layer for strategic-state oracle bounds, compatible-coalition hardness witnesses, bounded-dependence mechanism kernelization, policy surprise, reduced visibility dynamics, and binary belief repair.
- We evaluate trace-image encodings, phase controls, parameter-shift splits, IAAFT marginal/spectrum-matched nulls, raw, Fourier, recurrence-image, ROCKET-style time-series, and lightweight local-filter baselines, plus an external-trace adapter.

2 Related Work

El Farol, minority games, and congestion. Arthur’s El Farol problem uses a simple attendance threshold to show why a single deductive forecast can self-negate [2]. The minority game abstracts this into a repeated game in which success comes from being in the smaller group [7, 24]. Rosenthal’s congestion games show that finite games with resource congestion have pure Nash equilibria via a potential function [19]. EHMGS inherit this negative-frequency logic but make action awareness and observation horizon explicit state variables.

More options, worse outcomes. Braess’ paradox is the canonical warning that adding capacity or route choice can harm decentralized users [5, 16]. The informational Braess paradox is closer to the present paper: users with expanded information sets can experience higher equilibrium costs [1]. Our model is not a replacement for network Wardrop analysis. It is a compact agent-based counterpart for settings where the newly visible object is not just a road, but an action, opportunity, or belief target.

Bounded reasoning and desire. Human play often departs from exact equilibrium. Cognitive hierarchy models allow agents to reason at finite depths [6]; quantal response equilibrium replaces sharp best responses with noisy probabilistic responses [11, 15]. Prospect theory, the law of small numbers, gambler’s fallacy, and desirability bias show why a wanted outcome can affect probability judgment and prediction thresholds [8, 13, 20, 23]. EHMGS use these ideas modestly: desire is an additive preference term in perceived utility, not a claim that all probability distortion has one cause.

Epistemic limits. Epistemic models of games study how rationality, belief, and higher-order belief support solution concepts [18]. Common knowledge is central to coordination [21], while Aumann’s theorem shows how strong common-prior and common-knowledge assumptions constrain disagreement [4]. Unawareness models go further: players may fail to represent actions, players, or states at all [12]. EHMGS use this distinction to separate uncertainty about an outcome from absence of the outcome from an agent’s model.

Visual encodings of dynamics. Time-series imaging maps one-dimensional traces into spatial objects that can be read by visual inspection or image-analysis pipelines. Gramian angular fields and related maps were introduced for time-series classification and imputation [22]; recurrence plots visualize repeated states in a dynamical system [9]; and Fourier phase is a classical control variable for local image structure [17]. We use these tools conservatively: they are diagnostics for strategic trajectories, not a substitute for the formal model.

Disclosure optimization. Once visibility becomes a decision variable, the model touches standard algorithmic questions: choose which information to reveal, under what budget, and with what welfare or harm guarantees. The minimum harmful revelation task below is a covering problem in disguise, so the usual set-cover hardness phenomena are relevant [10, 14]. This connection makes the algorithmic layer part of the EHMGS core rather than a separate collection of complexity proxies.

3 Model

Let $N = \{1, \dots, n\}$ be agents and $A = \{1, \dots, K\}$ actions. At round t , agent i is aware of a nonempty subset $A_i(t) \subseteq A$. A public visibility shock is an update $A_i(t+1) \supseteq A_i(t)$ for a set of agents. We distinguish three information structures. A *private expansion* reveals an action to selected agents without making the event common knowledge. A *public revelation* makes the action visible to all agents and makes that visibility itself public. A *correlated disclosure* reveals to a subset whose membership is statistically related, for example through a platform, community, or recommendation channel. These structures can have different strategic effects even when the number of newly aware agents is the same. Formally, agent i 's perceived awareness share for action a is $\hat{\pi}_{i,a}$, a belief about how many other agents have a in their awareness sets. Private revelation changes A_i but need not change $\hat{\pi}_{j,a}$ for $j \neq i$. Public revelation sets $\hat{\pi}_{i,a} = 1$ for all agents and makes that event common knowledge. Correlated revelation gives agents a signal cell C_i and sets $\hat{\pi}_{i,a} = \mathbb{E}[|S|/n \mid C_i]$. Thus ‘‘I know a ’’, ‘‘I know others know a ’’, and ‘‘it is common knowledge that a is available’’ are different EHM states.

Proposition 1 (Correlated disclosure can differ at fixed reach). *Fix a focal action r and a recipient set S of size q . Compare two disclosures that reveal r to exactly the same agents in S . In the first, the recipient set is publicly announced, so each recipient uses $\hat{\pi}_{i,r}^P = q/n$. In the second, recipients observe only a correlated group signal C_i and use posterior $\hat{\pi}_{i,r}^C = p$. If $\eta > 0$, $p \neq q/n$, and all other perceived-utility terms are held fixed, then the logit odds of choosing r differ by*

$$\frac{\Pr_C(a_i = r)/\Pr_C(a_i = b)}{\Pr_P(a_i = r)/\Pr_P(a_i = b)} = \exp\left(\frac{\eta(q/n - p)}{\tau}\right)$$

against any common alternative $b \in A_i$. Hence two disclosures with the same number of newly aware agents can induce different adoption, target price-of-information, and welfare effects.

Proof. The two disclosures produce the same feasible action set for every agent, so they differ only through the awareness-share term in perceived utility. The correlated signal changes $\hat{u}_{i,r}$ relative to the public announcement by $\eta(q/n - p)$, while $\hat{u}_{i,b}$ is unchanged. The displayed odds ratio is the standard logit odds identity. If $p < q/n$, the correlated signal makes r appear more scarce and raises its adoption odds; if $p > q/n$, it lowers them. Because r 's realized payoff and welfare contribution depend on adoption, the induced equilibrium effects can differ even though the set of newly aware agents is identical. \square

Let $a_i(t) \in A_i(t)$ be the chosen action, and let

$$n_a(t) = \sum_{i=1}^n \mathbf{1}\{a_i(t) = a\}$$

be the crowd on action a . The realized payoff to agent i is

$$u_i(t) = v_{a_i(t)} - c \frac{n_{a_i(t)}(t)}{n},$$

where v_a is intrinsic value and $c > 0$ is the congestion coefficient. The experiments also use the more general congestion family

$$u_i(t) = v_{a_i(t)} - c \left(\frac{n_{a_i(t)}(t)}{n} \right)^\rho, \quad \rho > 0,$$

so the main mechanism is not tied to a linear cost curve.

Agents do not observe the full process. Each has a horizon h_i . Let $\hat{n}_{i,a}(t)$ be the mean realized count of action a in the last h_i rounds. The perceived utility used for choice is

$$\hat{u}_{i,a}(t) = v_a - c \frac{\hat{n}_{i,a}(t)}{n} + \eta(1 - \pi_a(t)) + \lambda_i d_{i,a}, \quad a \in A_i(t),$$

where $\pi_a(t) = n^{-1} \sum_i \mathbf{1}\{a \in A_i(t)\}$ is realized awareness share. In the information-structure version, agent i replaces this term by the perceived share $\hat{\pi}_{i,a}(t)$. The parameter $\eta \geq 0$ is an epistemic-scarcity bonus, and $\lambda_i d_{i,a}$ is the desire term. The desire term is reduced-form: it can represent a utility tilt, attention toward an action, or a prediction-threshold shift, but it is not meant to identify gambler's fallacy, optimism, arousal, and desirability bias as one mechanism. Actions outside $A_i(t)$ have perceived utility $-\infty$. Choices follow a quantal response:

$$\Pr(a_i(t) = a) = \frac{\exp(\hat{u}_{i,a}(t)/\tau)}{\sum_{b \in A_i(t)} \exp(\hat{u}_{i,b}(t)/\tau)}.$$

Definition 1 (Epistemic scarcity). *An action a has epistemic scarcity at time t when $\pi_a(t) < 1$. Its scarcity is not physical unavailability, but absence from some agents' action spaces.*

Definition 2 (Inverse abundance). *An action exhibits inverse abundance on an interval if increasing its awareness or adoption rate decreases its realized payoff.*

3.1 Awareness Transitions

Let

$$\mathcal{L} = \prod_{i=1}^n 2^A$$

be the finite awareness lattice ordered by componentwise inclusion. An awareness profile $\mathcal{A} = (A_1, \dots, A_n) \in \mathcal{L}$ records which actions are conceivable to each agent. For a focal action r , a private revelation to agent set $S \subseteq N$ is the join operator

$$R_S^r(\mathcal{A})_i = \begin{cases} A_i \cup \{r\}, & i \in S, \\ A_i, & i \notin S. \end{cases}$$

Public revelation is R_N^r , interpreted as both universal visibility and common observability of the revelation event. Correlated revelation is R_S^r where S is drawn from, or constrained by, a platform/community sigma-field. This separates the number of newly aware agents from the information structure by which they become aware.

For fixed \mathcal{A} , let $F_\tau(x; \mathcal{A})$ be the population logit response map induced by perceived utilities and congestion share x . A *mean-field awareness equilibrium* is a pair (x^*, \mathcal{A}^*) such that

$$x^* = F_\tau(x^*; \mathcal{A}^*), \quad \Gamma(\mathcal{A}^*, x^*) = \mathcal{A}^*,$$

where $\Gamma : \mathcal{L} \times \Delta(A) \rightarrow \mathcal{L}$ is an awareness transition operator.

Proposition 2 (Finite convergence of monotone awareness expansion). *Suppose Γ is inflationary: $\Gamma(\mathcal{A}, x) \succeq \mathcal{A}$ for every awareness profile and population state. Then every awareness trajectory $\mathcal{A}_{t+1} = \Gamma(\mathcal{A}_t, x_t)$ reaches an awareness fixed point after at most*

$$nK - \sum_{i=1}^n |A_i(0)|$$

strict expansion events, regardless of the intermediate population states x_t .

Proof. The lattice has one Boolean coordinate for each agent-action pair. Inflationary updates can flip a coordinate only from absent to present and never back. The displayed quantity is exactly the number of initially absent coordinates. Once no coordinate flips, Γ has reached an awareness fixed point. \square

Proposition 3 (Existence of mean-field awareness equilibrium). *Suppose Γ is inflationary and eventually stationary on every monotone awareness path. For every terminal awareness profile \mathcal{A} , if $F_\tau(\cdot; \mathcal{A})$ is continuous on the action simplex, then there exists a mean-field awareness equilibrium (x^*, \mathcal{A}^*) .*

Proof. By finite convergence, every monotone awareness path reaches some terminal profile \mathcal{A}^* with $\Gamma(\mathcal{A}^*, x) = \mathcal{A}^*$ for the relevant terminal states. The simplex is compact and convex, and F_τ is continuous because logit probabilities are continuous in utilities. Brouwer's theorem gives $x^* = F_\tau(x^*; \mathcal{A}^*)$. \square

Proposition 4 (Uniqueness under masked-logit contraction). *Fix an awareness profile and a finite collection of population types θ , each with mass w_θ , awareness mask M_θ , and masked-logit choice vector $p_\theta(x)$. Let*

$$F_\tau(x; \mathcal{A}) = \sum_{\theta} w_\theta p_\theta(x)$$

be the aggregate response map, where congestion enters utility through $-g_a(x_a)$. For each x , let $J_\theta(x)$ be the Jacobian of the masked softmax with respect to feasible-action utilities and let $D(x) = \text{diag}(g'_1(x_1), \dots, g'_K(x_K))$, with unavailable coordinates zeroed by M_θ . If

$$L = \sup_{x \in \Delta(A)} \left\| \sum_{\theta} w_\theta J_\theta(x) D(x) \right\|_{\infty} < 1,$$

then $F_\tau(\cdot; \mathcal{A})$ is a contraction in sup norm and has a unique fixed point. A simple sufficient condition for $g_a(x_a) = c_a x_a^\rho$, $\rho \geq 1$, is

$$\frac{\max_a c_a \rho}{2\tau} < 1,$$

because every masked-softmax Jacobian has ℓ_∞ operator norm at most $1/(2\tau)$. If $0 < \rho < 1$, the same statement holds on any region $x_a \geq \epsilon > 0$ after replacing $\max_a c_a \rho$ by $\max_a c_a \rho \epsilon^{\rho-1}$.

Proof. For a fixed awareness mask, unavailable actions have zero choice probability and zero utility derivative, so the usual softmax Jacobian applies on the feasible face of the simplex. The chain rule gives

$$\nabla_x F_\tau(x; \mathcal{A}) = - \sum_{\theta} w_\theta J_\theta(x) D(x).$$

The displayed operator bound implies $\|F_\tau(x; \mathcal{A}) - F_\tau(y; \mathcal{A})\|_{\infty} \leq L \|x - y\|_{\infty}$ by the mean-value theorem on the simplex. Banach's fixed-point theorem gives uniqueness. For a softmax row p , the absolute row sum of its utility Jacobian is $2p_a(1 - p_a)/\tau \leq 1/(2\tau)$, yielding the scalar sufficient condition. The ϵ -restricted nonlinear case uses $\max_a g'_a(x_a) \leq \max_a c_a \rho \epsilon^{\rho-1}$. \square

This condition is deliberately sufficient, not necessary. It covers the fixed-awareness logit phase, including heterogeneous masks and action-specific congestion slopes, but it does not rule out multiple fixed points when temperature is low, congestion is steep, or awareness itself is still moving. Those cases are handled experimentally as sensitivity regimes rather than claimed as globally unique equilibria.

Proposition 5 (Sensitivity to revelation size). *Under the contraction condition above, let $\mathcal{A}' = R_{\zeta}^r(\mathcal{A})$ reveal action r to $q = |S \setminus \{i : r \in A_i\}|$ newly aware agents. If the direct effect of changing the masks of these agents is at most q/n in the aggregate logit response, then the fixed points satisfy*

$$\|x^*(\mathcal{A}') - x^*(\mathcal{A})\|_{\infty} \leq \frac{q/n}{1-L}.$$

In particular, the revealed action's equilibrium share can rise by at most this amount.

Proof. Let F and F' be the two response maps. At the old fixed point x^* , changing availability for q of n agents can change the population-average response by at most q/n . For the new fixed point x'^* ,

$$\|x'^* - x^*\|_{\infty} \leq \|F'(x'^*) - F'(x^*)\|_{\infty} + \|F'(x^*) - F(x^*)\|_{\infty} \leq L\|x'^* - x^*\|_{\infty} + q/n.$$

Rearranging proves the bound. \square

Proposition 6 (Nonlinear price-of-information bound and tightness). *Let $g_r(x) = cx^{\rho}$, and suppose revelation raises the equilibrium share of the focal action from x to $x + \delta$. The target price of information is*

$$P_r = c((x + \delta)^{\rho} - x^{\rho}).$$

For $\rho \geq 1$,

$$c\rho x^{\rho-1}\delta \leq P_r \leq c\rho(x + \delta)^{\rho-1}\delta.$$

Combining with the sensitivity proposition gives

$$P_r \leq c\rho \left(x + \frac{q/n}{1-L}\right)^{\rho-1} \frac{q/n}{1-L}.$$

The upper bound is tight in the zero-temperature limit when every newly aware agent selects r . If revelation causes no new adoption, then $P_r = 0$, so visibility alone is not sufficient.

Proof. The exact expression follows by subtracting post- and pre-revelation congestion payoffs. The two inequalities are the mean-value theorem applied to $\xi \mapsto c\xi^{\rho}$, whose derivative is increasing for $\rho \geq 1$. The sensitivity substitution gives the displayed bound. In the deterministic limit, $\delta = q/n$ whenever all newly aware agents choose the revealed action, so the bound is attained up to the contraction slack; if $\delta = 0$, the exact expression gives zero. \square

Proposition 7 (Dynamic awareness is not reducible to a static count game). *Assume $\eta > 0$ or at least one agent's feasible set changes under revelation. There is no static congestion game whose payoffs and logit response depend only on current action counts and fixed feasible action sets that matches EHMG one-step behavior for all histories. In particular, two EHMG histories can have the same realized count vector x but different awareness profiles $\mathcal{A} \neq \mathcal{A}'$, and hence different next-period logit responses after a revelation operator.*

Proof. A static count-based congestion game assigns the same utilities and the same logit response to any two histories with the same current count vector. EHMG does not: the perceived utility contains $\eta(1 - \pi_r)$, and the action mask $\mathbf{1}\{r \in A_i\}$ changes when revelation occurs. Thus two histories with identical realized counts but different π_r or different agent masks generate different response probabilities for r . A fixed smaller action space can match one awareness profile, but it cannot simultaneously match both profiles and the transition between them. \square

Proposition 8 (Count-equivalent histories can have different next choices). *Let $N = \{1, 2\}$, $A = \{b, r\}$, $v_b = v_r = 0$, $c = 0$, $\eta > 0$, and temperature $\tau > 0$. Consider two histories with the same current count vector $n_b = 2, n_r = 0$. In history H , $A_1 = \{b, r\}$ and $A_2 = \{b\}$, so $\pi_r = 1/2$. In history H' , $A_1 = A_2 = \{b, r\}$, so $\pi_r = 1$. Then the next-period logit probabilities for action r differ:*

$$\Pr_H(a_1 = r) = \frac{\exp(\eta/(2\tau))}{1 + \exp(\eta/(2\tau))}, \quad \Pr_H(a_2 = r) = 0,$$

whereas

$$\Pr_{H'}(a_1 = r) = \Pr_{H'}(a_2 = r) = \frac{1}{2}.$$

Thus a model observing only the current count vector cannot match EHM transition kernels across awareness profiles.

Proof. Both histories have the same realized counts and the same intrinsic action values. They differ only in awareness. In H , agent 1 receives scarcity bonus $\eta(1 - \pi_r) = \eta/2$ for r , while agent 2 cannot choose r . In H' , both agents can choose both actions and the scarcity bonus is zero. Substituting these utilities into the logit formula gives the stated probabilities. \square

Proposition 9 (Fixed-awareness EHM is a congestion potential game). *Fix awareness sets A_i and let payoffs be $u_i(a) = v_{a_i} - g_{a_i}(n_{a_i}(a))$, where each g_a depends only on the number of agents choosing a . Then the finite EHM stage game is an exact potential game on the restricted strategy spaces A_i , with potential*

$$\Phi(a) = \sum_{b \in A} \sum_{m=1}^{n_b(a)} (v_b - g_b(m)).$$

Proof. Consider a unilateral deviation by agent i from x to y . Only counts on x and y change. The change in Φ removes the marginal term $v_x - g_x(n_x)$ and adds $v_y - g_y(n_y + 1)$, exactly matching the deviator's payoff change. Awareness only restricts which deviations are feasible; it does not alter the potential identity. \square

Proposition 10 (Stationary logit revision under fixed awareness). *For fixed awareness sets and asynchronous logit revision with temperature $\tau > 0$, the induced Markov chain over feasible action profiles has stationary distribution*

$$\mu_\tau(a) = \frac{\exp(\Phi(a)/\tau)}{\sum_{a'} \exp(\Phi(a')/\tau)}.$$

Thus fixed-awareness EHM inherits the standard regularized equilibrium structure of finite potential games.

Proof. In an exact potential game, the logit transition ratio between two profiles that differ by one agent equals $\exp((\Phi(a') - \Phi(a))/\tau)$. This is the detailed-balance condition for the Gibbs measure above. Since the finite chain has positive probability on all feasible unilateral revisions, the stationary distribution is unique on the feasible profile graph. \square

Proposition 11 (Visibility can destroy the payoff it reveals). *Suppose action a has realized payoff $u_a(n_a) = v_a - cn_a/n$ with $c > 0$. If a visibility shock increases its realized crowd from n_a to $n'_a > n_a$ while v_a and c are fixed, then the action payoff falls by*

$$u_a(n_a) - u_a(n'_a) = c \frac{n'_a - n_a}{n} > 0.$$

Proof. Substitute the two crowd levels into the payoff function and subtract. The strict inequality follows from $c > 0$ and $n'_a > n_a$. \square

Proposition 12 (A welfare condition for harmful revelation). *Under linear congestion, suppose a visibility expansion moves m agents from action b to a newly revealed action r , with pre-shock counts n_b and n_r . Aggregate welfare decreases whenever*

$$\frac{2c}{n}(n_r - n_b + m) > v_r - v_b.$$

Proof. Total welfare is $W = \sum_a n_a v_a - \frac{c}{n} \sum_a n_a^2$. The move changes only actions b and r . Hence

$$\Delta W = m(v_r - v_b) - \frac{c}{n} [(n_r + m)^2 - n_r^2 + (n_b - m)^2 - n_b^2],$$

which simplifies to

$$\Delta W = m(v_r - v_b) - \frac{2cm}{n}(n_r - n_b + m).$$

For $m > 0$, $\Delta W < 0$ exactly under the stated condition. \square

Proposition 13 (Monotone response informational-loss condition). *Let a response rule assign a weakly larger probability to action r whenever its perceived utility increases and all other perceived utilities are fixed. If a public revelation of r weakly increases its perceived utility for at least one newly aware agent and strictly increases expected adoption of r , then every strictly decreasing realized payoff $u_r(n_r)$ yields a strictly lower expected payoff for action r after revelation.*

Proof. The response assumption implies that the post-revelation adoption count of r first-order stochastically dominates the pre-revelation count and is strictly larger with positive probability. Since u_r is strictly decreasing in the count, taking expectations reverses the order. \square

Definition 3 (Price of information). *For focal action r , awareness profile \mathcal{A} , and revelation set S , define the target price of information as*

$$P_r(S; \mathcal{A}) = u_r(x_r(\mathcal{A})) - u_r(x_r(R_S^r(\mathcal{A}))),$$

where $x(\mathcal{A})$ is the fixed-awareness mean-field logit equilibrium. Under linear congestion this is exactly

$$P_r(S; \mathcal{A}) = c(x_r(R_S^r(\mathcal{A})) - x_r(\mathcal{A})).$$

Proposition 14 (Target price and welfare can disagree). *Under linear congestion with unit population mass, let a disclosure move δ mass from action b to focal action r . The target price is $P_r = c\delta$, while welfare changes by*

$$\Delta W = \delta(v_r - v_b) - c[(x_r + \delta)^2 - x_r^2 + (x_b - \delta)^2 - x_b^2].$$

Consequently the target price of information is not an aggregate welfare measure. With $c = 1$, $x_r = 0.1$, $x_b = 0.9$, $\delta = 0.2$, and $v_r - v_b = 1$, one obtains $P_r = 0.2$ and $\Delta W = 0.44 > 0$. With $x_r = 0.8$, $x_b = 0.2$, $\delta = 0.1$, and $v_r = v_b$, one obtains $P_r = 0.1$ and $\Delta W = -0.14 < 0$. Finally, from the same baseline $(x_r, x_b, x_d) = (0.1, 0.6, 0.3)$ with $c = 1$, $(v_r, v_b, v_d) = (2.0, 1.9, 1.0)$, policy S moving 0.1 mass from b to r has $P_r(S) = 0.1$ and $\Delta W(S) = 0.09$, while policy T moving 0.2 mass from d to r has $P_r(T) = 0.2$ and $\Delta W(T) = 0.20$. Minimizing target price prefers S , but maximizing aggregate welfare prefers T .

Proof. The expression follows by subtracting pre- and post-disclosure welfare $\sum_a x_a v_a - c \sum_a x_a^2$. The numerical claims are direct substitutions. The examples show that target payoff loss can coexist with welfare gain, welfare loss, or policy rankings opposite to welfare rankings. \square

Definition 4 (Budgeted welfare-safe disclosure). *Given candidate disclosure groups G_1, \dots, G_m , budget B , welfare floor \underline{W} , and awareness profile \mathcal{A} , choose $I \subseteq \{1, \dots, m\}$ with $|I| \leq B$ to maximize newly aware agents subject to*

$$W(R_{\cup_{j \in I} G_j}^r(\mathcal{A})) \geq \underline{W}.$$

Definition 5 (Minimum harmful revelation). *Given candidate groups and a target price threshold γ , find a minimum cardinality index set I such that*

$$P_r(\cup_{j \in I} G_j; \mathcal{A}) \geq \gamma.$$

Proposition 15 (Minimum harmful revelation is NP-hard). *Minimum harmful revelation is NP-hard, even when all candidate groups reveal the same focal action.*

Proof. Reduce from set cover. Let the set-cover universe be $U = \{1, \dots, n\}$ and let the candidate sets be $\mathcal{S}_1, \dots, \mathcal{S}_m$. Build an EHMG instance with one agent per element of U , one default action b , and one focal action r . Initially every agent is aware only of b . Candidate disclosure group G_j reveals r exactly to the agents corresponding to \mathcal{S}_j . Choose $v_r - v_b$ large enough and temperature small enough that every newly aware agent strictly selects r in the deterministic best-response limit, while unaware agents cannot select r . With $g_r(x) = cx^\rho$, revealing a family I therefore makes the equilibrium share of r equal to

$$x_r(I) = \frac{|\cup_{j \in I} \mathcal{S}_j|}{n}.$$

Set the harmful threshold to

$$\gamma = c(1^\rho - 0^\rho) = c.$$

Then $P_r(I) \geq \gamma$ if and only if $\cup_{j \in I} \mathcal{S}_j = U$. Thus a minimum harmful revelation is exactly a minimum set cover. The construction is polynomial. The same argument with $\gamma = c(k/n)^\rho$ gives partial-cover hardness for a k -agent harmful threshold. For positive but sufficiently small logit temperature, strict utility separation preserves the reduction by continuity with a fixed margin. \square

Proposition 16 (A normalized Braess visibility loss). *Consider a unit demand network with edges $s \rightarrow x$ of cost f , $x \rightarrow t$ of cost 1, $s \rightarrow y$ of cost 1, and $y \rightarrow t$ of cost f . Without edge $x \rightarrow y$, the Wardrop equilibrium splits flow equally and has cost 1.5. If the zero-cost edge $x \rightarrow y$ is visible and usable, the Wardrop equilibrium sends all flow along $s \rightarrow x \rightarrow y \rightarrow t$ and has cost 2.0.*

Proof. Without the middle edge, the two route costs are $x_1 + 1$ and $1 + x_2$, with $x_1 + x_2 = 1$. Wardrop equilibrium equalizes them at $x_1 = x_2 = 0.5$, yielding cost 1.5. With the middle edge, the zig-zag route has cost $(x_1 + x_3) + (x_2 + x_3)$, where x_3 is zig-zag flow. At $x_3 = 1$ and $x_1 = x_2 = 0$, all available routes have cost at least 2, and the used route has cost 2. No user can improve by deviating, so this is a Wardrop equilibrium with higher cost. \square

Proposition 17 (EHMG revelation strictly raises information-constrained Wardrop cost). *Embed the normalized Braess network as an EHMG in which routes are actions and route awareness is the feasible action set. Initially all agents are aware only of the two outer routes, so the information-constrained Wardrop equilibrium has cost 1.5. A public revelation operator that makes the zero-cost middle edge common knowledge expands every feasible route set to include the zig-zag route. The resulting Wardrop equilibrium has cost 2.0. Hence EHMG public revelation strictly increases equilibrium congestion cost by 0.5.*

Proof. The initial awareness profile restricts every agent to the two-route subgame, whose Wardrop equilibrium is the equal split from the previous proposition and has cost 1.5. Public revelation is R_N^r for the zig-zag route r : every agent can now choose it and every agent observes that all others can choose it. The full route set is exactly the Braess network with the middle edge available, whose Wardrop equilibrium sends all flow through the zig-zag route at cost 2.0. The same physical network and demand are used in both states; only the awareness-transition operator changes the equilibrium. \square

4 Experiments

All experiments are generated by `scripts/materialize_experiments.py`. The script writes raw and aggregate CSV files, selected manuscript figures, auxiliary plot previews, an experiment JSON audit, and a reproducibility manifest. The source package includes code and result artifacts.

E1: awareness sweep. We vary initial awareness of a hidden third action from 0.03 to 1.00. Each condition uses 24 deterministic-seed replicates of a 501-agent, 280-round game. The outcome is the hidden action’s late-window payoff and choice rate.

E2: public visibility shock. The hidden action begins with 8% awareness. At round 180, it is revealed to all agents. We compare desire biases 0.00, 0.20, and 0.45, using 18 replicates per condition. The primary outcomes are hidden-action payoff collapse, hidden-action choice-rate jump, and welfare change.

E3: horizon–desire grid. We cross horizons $h \in \{1, 3, 8, 20\}$ with desire biases $\lambda \in \{0, 0.12, 0.28, 0.45\}$. All agents know all actions, so this experiment isolates bounded horizon and desire from awareness. The outcome is late-window volatility of the focal action’s choice rate.

E4: Braess information comparison. We compute the analytic normalized Braess costs from the Braess visibility proposition and write the restricted and full-information route flows to CSV.

E5: transferred algorithmic mechanism layer. We materialize the general-purpose code layer behind the simulations in formal mechanism language. The layer includes binary oracle identification bounds, a k-Clique to compatible-coalition reduction, min-fill mechanism graph kernelization, bounded-treewidth dynamic-programming work estimates, risk-plus-ambiguity policy scoring, message-passing repair for binary belief consistency checks, and a reduced strategic SDE over salience, dispersion, and delay pressure.

E6: robustness phase diagram. To separate structural behavior from parameter-induced behavior, we repeat the visibility shock with no desire bias and no direct desire term. We vary temperature $\tau \in \{0.08, 0.16, 0.32, 0.64\}$, congestion curvature $\rho \in \{0.75, 1, 1.5, 2\}$, and learning rule $\{\text{softmax}, \text{epsilon-greedy}\}$. The outcome is the post-revelation payoff collapse of the revealed action and welfare change.

E7: disclosure and desire-as-attention. We compare no revelation, private partial revelation, correlated partial disclosure, public common revelation, desire acting through attention/awareness, and desire acting through utility. This addresses the behavioral-identification concern: desire can influence which action is represented, not only how a represented action is valued.

E8: counterfactual baselines. We compare the public EHM shock with ordinary full-awareness congestion, full-awareness minority dynamics without epistemic scarcity, private partial revelation, and public revelation without the scarcity bonus. This tests whether the EHM formalism predicts behavior absent from standard baselines.

E9: disclosure optimization. We instantiate budgeted welfare-safe disclosure and minimum harmful revelation on a six-group disclosure instance. Exact enumeration, greedy selection, full public revelation, and the minimum harmful subset are all evaluated under the same mean-field logit outcome map.

E10: strategic trajectory imaging. We encode the public-visibility-shock trace as a line image, Gramian-angular hidden-rate image, recurrence image, Gramian payoff image, invertible spectral carrier, and phase-scrambled control.

E11: trace-image recognition and stress benchmark. We generate four labeled strategic regimes—ordinary congestion, epistemic scarcity, public revelation, and attention-mediated discovery—with deterministic train/test splits over seeds. A nearest-centroid classifier is evaluated on raw trace features, Fourier features, recurrence-image features, and the full image bundle. We then run a harder binary stress benchmark: every awareness-cascade trace is paired with an iterative amplitude-adjusted Fourier-transform (IAAFT) null that preserves the trace’s sorted values and approximately preserves its Fourier magnitudes. The train and test splits differ in reveal time, temperature, congestion curvature, horizon distribution, action-value gap, circular phase, and noise. Raw positions, Fourier magnitudes, a ROCKET-style random-convolution time-series baseline, recurrence-image summaries, an image-structure bundle, and a small local-filter baseline trained from scratch are evaluated. Additional CSV checks vary image resolution, recurrence threshold, Gramian variant, spectral-carrier construction, and phase scrambling; metadata-only and marginal-only leakage probes test seed, trace-length, reveal-time, parameter, and marginal-statistic shortcuts.

E12: external-trace adapter. No real external trace dataset is included. Instead, the code provides a long-format CSV adapter for future route-choice, online-attention, experimental-minority-game, or gambling-prediction traces, plus a synthetic external generator with cascade and cyclic dynamics that do not call the EHM simulator. The canonical required columns are `trace_id`, `time`, `signal_name`, and `value`; optional columns record label, group, and metadata. The reproducibility script writes both a long-format adapter input and a smoke-test summary with 16 traces.

5 Results

The awareness sweep is reported textually rather than as a manuscript figure. The hidden-action payoff falls with fitted slope -0.418 , moving from 1.152 at the lowest awareness level to 0.755 under full awareness. This supports the inverse abundance claim in its simplest form: the hidden action is not valuable merely because $v_C > v_A = v_B$; it is valuable because too few agents can select it. When awareness approaches one, its crowd increases and its advantage decays.

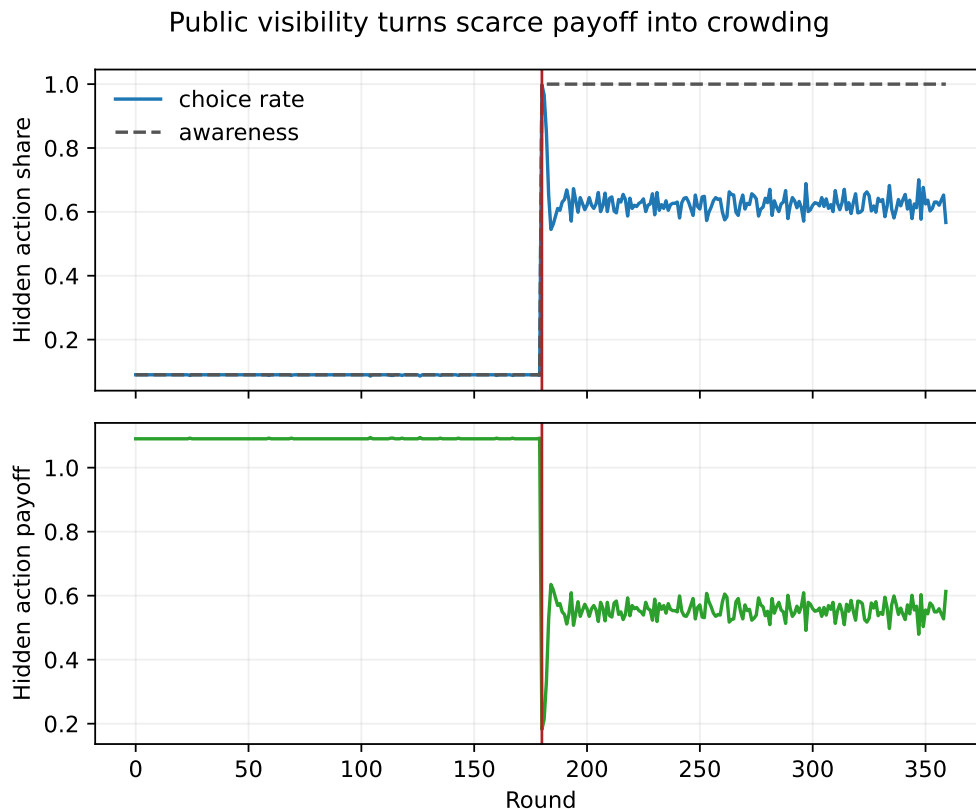


Figure 1: A public revelation shock makes the hidden action common and crowded. In the strong desire condition, the hidden-action choice rate rises by 0.545, while hidden-action payoff falls by 0.545.

Figure 1 shows the mechanism dynamically. Before revelation, the hidden action has low awareness and high realized payoff. After revelation, the same action is selected by more agents. Desire accelerates the movement toward the revealed action, converting epistemic scarcity into crowding.

The horizon–desire grid isolates bounded observation and desire without using another figure: focal-action volatility ranges from 0.022 to 0.495, and shorter horizons with stronger desire produce larger oscillations. The normalized Braess comparison is also reported directly: route-set expansion raises equilibrium cost from 1.500 to 2.000, an increase of 0.500.

The reduced strategic dynamics and algorithmic-transfer checks are retained as auditable generated artifacts rather than manuscript figures. Their CSV record reports 9 oracle queries for 501 strategic states, 6 Fano-limited observations in an eight-class task, a treewidth reduction from 5 to 2, policy surprise 0.664, policy expected success 0.709, and 0 remaining belief-consistency violations.

The robustness and disclosure-mode checks are likewise kept textual. With desire removed, the revealed action’s payoff collapse remains positive in 1.000 of raw grid cells, with raw collapses ranging from 0.141 to 0.406. Public common revelation produces payoff collapse 0.333; desire-as-attention changes hidden-action choice rate by 0.007, while direct desire-as-utility changes it by 0.550. These comparisons keep the behavioral identification claim without adding near-duplicate charts.

The counterfactual baselines are also reported without a separate bar chart. The EHMG public revelation condition produces hidden-action payoff collapse 0.340, while the ordinary full-awareness congestion baseline changes by only 0.000, giving epistemic gap 0.339. This addresses the main

experimental criticism: the mechanism is not merely “more users of a congestible action lowers its payoff.” In the ordinary full-awareness baseline there is no hidden action to reveal, so the same pre/post measurement is essentially flat. Public revelation without the scarcity bonus still collapses payoff by 0.335, showing that action-space expansion itself is doing work.

Formal audit experiments. Four CSV-backed audit experiments make the theorem claims easier to inspect. The non-reducibility witness holds current action counts fixed but changes awareness masks, producing transition-kernel total variation 0.250 and aggregate revealed-action probability gap 0.134. The masked-logit audit evaluates 48 finite cases and records 10 cases where the sufficient scalar bound fails while the measured local Jacobian remains contractive; the largest measured local norm is 4.067. The price/welfare grid includes 3 welfare-increasing and 1 welfare-decreasing target-price cases, with 1 policy pair where minimizing target price and maximizing welfare disagree. The same-reach signal example holds recipient reach fixed while posterior awareness beliefs vary, yielding adoption spread 0.284 and relative-odds range $[0.407, 1.822]$. These audits are diagnostic checks on the formal distinctions, not substitutes for the proofs.

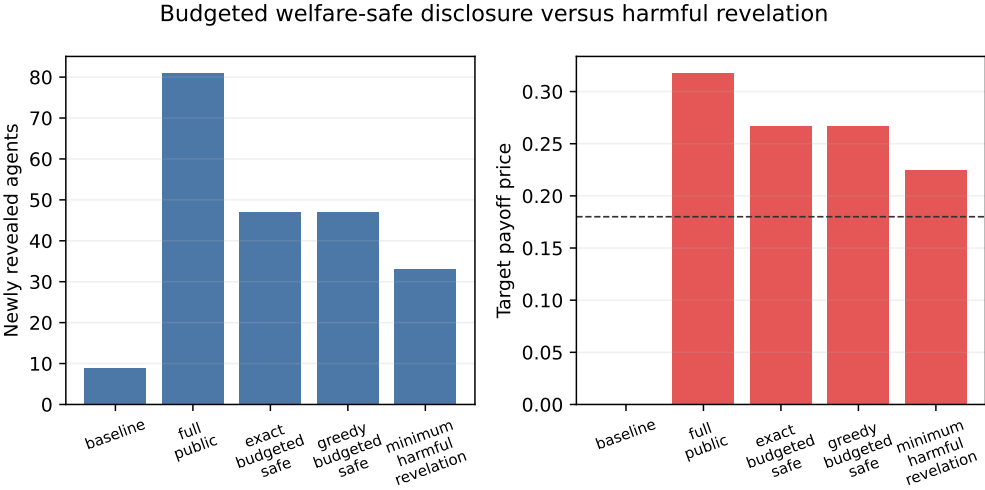


Figure 2: Algorithmic disclosure tasks. Exact budgeted welfare-safe disclosure reveals 47 agents, the greedy policy reveals 47, and the greedy gap is 0. Full public revelation has target price 0.318, while minimum harmful revelation crosses the target-price threshold with 2 groups and price 0.225.

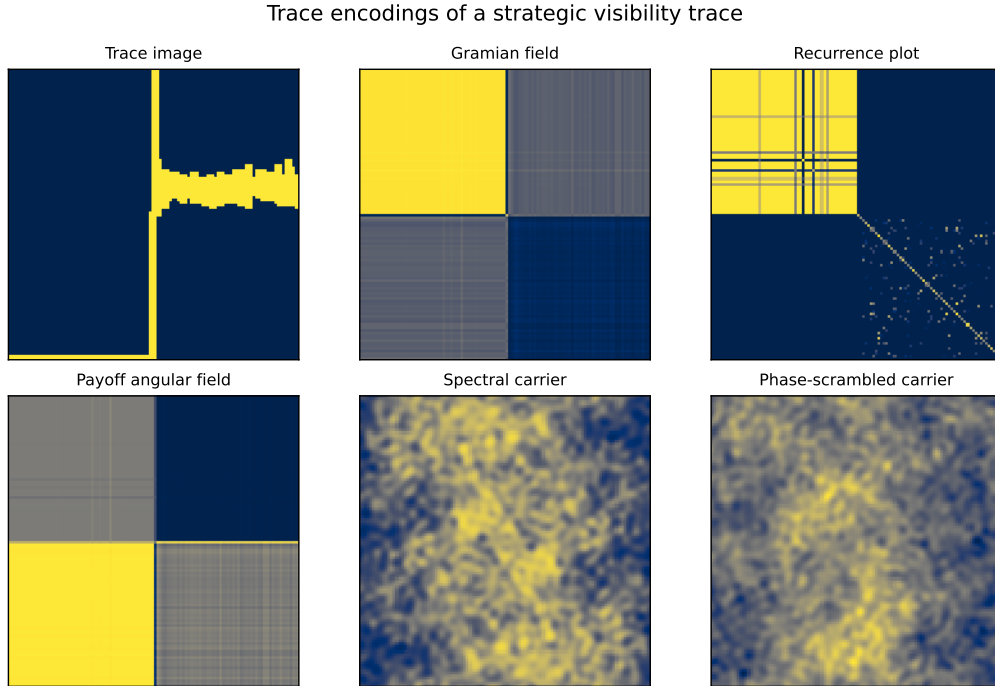


Figure 3: Trace encodings of one strategic trajectory. The six-panel diagnostic includes a trace image, Gramian and recurrence images, a payoff angular field, an invertible spectral carrier, and a phase-scrambled carrier. The spectral carrier reconstructs the z-scored hidden-rate trace at 59.9 dB after 8-bit quantization; the phase control changes local structure by 0.034 while leaving the normalized radial power profile close, with relative error 0.000.

Figure 3 shows the image representations used by the trace recognition benchmark. The figure is not the evidence by itself; it records what the feature pipelines see before the held-out detection task.

The basic four-regime recognition task is reported without a separate bar chart: over 40 held-out traces, raw and Fourier baselines reach 1.000 and 1.000, recurrence-image features reach 1.000, and the image bundle reaches 1.000. Because this task is partially separable from raw trajectories, the stricter matched-null benchmark is reported textually rather than as another bar chart. The matched null removes the easy marginal and spectral cues, and the test split changes the event location and game parameters. Raw trace features reach 0.542, Fourier magnitudes reach 0.479, the ROCKET-style time-series baseline reaches 0.583, recurrence-image summaries reach 0.604, and the image-structure bundle reaches 0.958. The small local-filter model reaches 0.604. The image-encoding gain over the best non-image baseline, including ROCKET, is 0.375. The ablation table reports 7 image-encoding controls, and the metadata-only leakage probe obtains 0.500, consistent with the paired cascade/null construction rather than a seed or parameter shortcut.

The remaining generated quantities are in the CSV tables and JSON experiment summary; the manuscript avoids a large catch-all summary table.

6 Interpretation

Gambling. In a pure lottery, previous independent outcomes do not change the next draw. Yet gambling decisions are rarely pure computations of objective probability. They are threshold deci-

sions under arousal, loss framing, pattern search, and desire. EHMG represents this by separating realized payoff from perceived utility. Desire does not need to rewrite the true probability; it only needs to shift a borderline action into the chosen set.

The forest horizon. An agent in a forest can feel locally complete while being globally uninformed. This is not irrationality by itself. It is horizon-bounded rationality: the agent acts coherently inside the events represented in the local model. EHMG formalizes this as $A_i(t)$ and h_i . The world can contain actions and states that the agent neither observes nor evaluates.

Unobservable domains. Claims about domains outside observation should not be modeled as if all agents share one exhaustive state space and merely disagree about probabilities. In many cases, agents fill different state spaces. EHMG does not adjudicate metaphysical truth. It provides a formal language for the fact that agents can coordinate, disagree, or fragment because their horizons and awareness sets differ.

Formal epistemic status. The present model is a lattice model of action awareness, not a full epistemic logic with hierarchies of subjective state spaces. Public revelation is modeled as a lattice jump that is common to the population; private and correlated revelations are different transition operators on the same lattice. This is deliberately weaker than a complete game-with-unawareness foundation, but stronger than treating unawareness as a static omitted action.

Strategic value. The slogan “what is many is little; what is little is many” becomes precise: an action’s strategic value is a function of intrinsic value, crowding, and visibility. When a hidden action is rare in awareness, it can yield high payoff. When it becomes common knowledge, it can lose the very advantage that made it attractive.

7 Limitations

The model is deliberately minimal. It does not estimate parameters from human subjects, does not claim that desire is the only source of gambling bias, and does not replace equilibrium analysis in network games. It also does not give a complete epistemic-logic treatment of awareness hierarchies; the contribution is the awareness-transition game and disclosure-optimization layer. The simulations are agent-based stress tests for a proposed mechanism. The trace-encoding experiments establish trace-to-image structure under controlled synthetic game traces; they include a lightweight local-filter baseline but do not yet evaluate large image models, real video, or human-generated strategic trajectories. Future work should fit the model to experimental minority-game play, online attention cascades, route choice data, or gambling tasks in which predictions and likelihood judgments are separately elicited, and should test whether the matched-null trace-encoding result transfers through the external-trace adapter.

8 Conclusion

Epistemic horizon minority games turn a philosophical intuition into a testable formal object. Agents choose inside bounded horizons, awareness evolves on a finite lattice, some actions are valuable because few agents see them, desire can push marginal choices toward crowding, and common visibility can erase strategic payoff. The added disclosure tasks make the mechanism algorithmic:

one can ask which revelation policy is safe, which small revelation is harmful, and which traces reveal the underlying regime. The result is a compact formal and computational account of why, in strategic environments, abundance can reduce value and scarcity can expand it.

References

- [1] Daron Acemoglu, Ali Makhdoumi, Azarakhsh Malekian, and Asuman Ozdaglar. Informational Braess' paradox: The effect of information on traffic congestion. *Operations Research*, 66(4): 893–917, 2018. doi: 10.1287/opre.2017.1712.
- [2] W. Brian Arthur. Inductive reasoning and bounded rationality. *American Economic Review*, 84(2):406–411, 1994.
- [3] W. Brian Arthur. The El Farol bar problem. <https://sites.santafe.edu/~wbarthur/elfarol.htm>, 2022.
- [4] Robert J. Aumann. Agreeing to disagree. *The Annals of Statistics*, 4(6):1236–1239, 1976. doi: 10.1214/aos/1176343654.
- [5] Dietrich Braess. Über ein paradoxon aus der verkehrsplanung. *Unternehmensforschung*, 12: 258–268, 1968.
- [6] Colin F. Camerer, Teck-Hua Ho, and Juin-Kuan Chong. A cognitive hierarchy model of games. *Quarterly Journal of Economics*, 119(3):861–898, 2004. doi: 10.1162/0033553041502225.
- [7] Damien Challet and Yi-Cheng Zhang. Emergence of cooperation and organization in an evolutionary game. *Physica A: Statistical Mechanics and its Applications*, 246(3–4):407–418, 1997. doi: 10.1016/S0378-4371(97)00419-6.
- [8] Rachel Croson and James Sundali. The gambler's fallacy and the hot hand: Empirical data from casinos. *Journal of Risk and Uncertainty*, 30(3):195–209, 2005. doi: 10.1007/s11166-005-1153-2.
- [9] Jean-Pierre Eckmann, S. Oliffson Kamphorst, and David Ruelle. Recurrence plots of dynamical systems. *Europhysics Letters*, 4(9):973–977, 1987. doi: 10.1209/0295-5075/4/9/004.
- [10] Uriel Feige. A threshold of $\ln n$ for approximating set cover. *Journal of the ACM*, 45(4): 634–652, 1998. doi: 10.1145/285055.285059.
- [11] Jacob K. Goeree, Charles A. Holt, and Thomas R. Palfrey. Stochastic game theory for social science: A primer on quantal response equilibrium. *Working paper*, 2018.
- [12] Aviad Heifetz, Martin Meier, and Burkhard C. Schipper. Unawareness, beliefs and games. *Working paper*, 2006.
- [13] Daniel Kahneman and Amos Tversky. Prospect theory: An analysis of decision under risk. *Econometrica*, 47(2):263–291, 1979. doi: 10.2307/1914185.
- [14] Richard M. Karp. Reducibility among combinatorial problems. In *Complexity of Computer Computations*, pages 85–103. Plenum Press, 1972.
- [15] Richard D. McKelvey and Thomas R. Palfrey. Quantal response equilibria for normal form games. *Games and Economic Behavior*, 10(1):6–38, 1995. doi: 10.1006/game.1995.1023.

- [16] Anna Nagurney and Ladimer S. Nagurney. The Braess paradox. *International Encyclopedia of Transportation*, 2020.
- [17] Alan V. Oppenheim and Jae S. Lim. The importance of phase in signals. *Proceedings of the IEEE*, 69(5):529–541, 1981. doi: 10.1109/PROC.1981.12022.
- [18] Eric Pacuit and Olivier Roy. Epistemic foundations of game theory. In Edward N. Zalta and Uri Nodelman, editors, *The Stanford Encyclopedia of Philosophy*. 2025.
- [19] Robert W. Rosenthal. A class of games possessing pure-strategy Nash equilibria. *International Journal of Game Theory*, 2(1):65–67, 1973. doi: 10.1007/BF01737559.
- [20] Amos Tversky and Daniel Kahneman. Belief in the law of small numbers. *Psychological Bulletin*, 76(2):105–110, 1971. doi: 10.1037/h0031322.
- [21] Peter Vanderschraaf and Giacomo Sillari. Common knowledge. In Edward N. Zalta and Uri Nodelman, editors, *The Stanford Encyclopedia of Philosophy*. 2022.
- [22] Zhiguang Wang and Tim Oates. Imaging time-series to improve classification and imputation. In *Proceedings of the 24th International Joint Conference on Artificial Intelligence*, pages 3939–3945, 2015.
- [23] Paul D. Windschitl, Andrew R. Smith, Jason P. Rose, and Zlatan Krizan. The desirability bias in predictions: Going optimistic without leaving realism. *Organizational Behavior and Human Decision Processes*, 111(1):33–47, 2010. doi: 10.1016/j.obhdp.2009.08.003.
- [24] Chi Ho Yeung and Yi-Cheng Zhang. Minority games. *Encyclopedia of Complexity and Systems Science*, pages 5588–5604, 2009.